Characterization of Radiation Induced Color Centers in Lithium Fluoride

Abhiram Sharma[1], Patrick Huber[2], and Sam Hedges[2]

[1]School of Physics, Georgia Institute of Technology, Atlanta, GA, USA

[2]Center for Neutrino Physics, Department of Physics, Virginia Polytechnic Institute, VA, USA

Abstract

Interactions between energetic particles and a crystal's lattice structure can lead to observable vacancies in the crystal. In some materials, these vacancies are optically active (aka color centers), thus allowing one to determine the type and trajectory of particles that damage the crystal by fluorescence measurements. Lithium fluoride (LiF) is a particularly good candidate as an effective passive particle detector due to the relatively light masses of the Li and F ions, allowing for more energetic recoil tracks to be created within the crystal from particle interactions [2]. We have studied the bulk fluorescence of LiF after irradiation by neutrons and gamma rays by characterizing the time and temperature dependence of the fluorescence. These studies are useful in understanding how the history of LiF impacts its fluorescence. Using Light-Sheet Fluorescence Microscopy (LFSM), we also imaged single-site vacancies and damage tracks in 3 dimensions to study single particle interactions.

1. Introduction

Color centers are irregularities in a crystal's regular lattice structure which can alter its optical properties. High energy particles like neutrons and gamma rays can create these optical defects in certain materials. Recently, this principle has motivated the use of color center damage to detect low energy nuclear recoil events, which dark matter may participate in (PALEOCCENE) [1]. LiF is a primary candidate for this type of detector as previous studies have shown its high detection efficiency [2]. With improved characterization of how radiation damage influences color center formation in semi-pure, artificial LiF samples; long-lived natural samples of more commonly occurring minerals could eventually be scanned for evidence of dark matter interactions accumulated over 10^6 to 10^9 years [1]. In this study, we will characterize the impact of LiF's temporal and thermal history on color center fluorescence after gamma and neutron irradiation. These measurements were done with a spectrophotometer. Additionally, data from samples measured by a benchtop mesoSPIM was processed to evaluate individual particle damage tracks in the crystals.

2. Theory

2.1. LiF Color Centers

F-centers are a specific type of color center where anionic vacancies get filled with electrons, which can then be excited and re-emit light at different wavelengths.

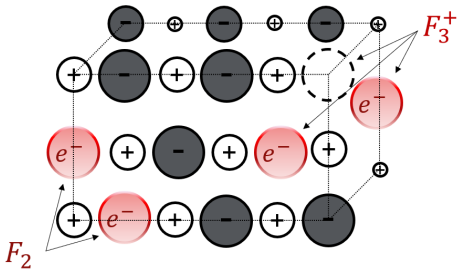

Figure 1: LiF Color Center Diagram

In this study of LiF, the two types of color centers of interest are F_2 centers (2 adjacent vacancies filled with 2 electrons) and F_3^+centers (3 adjacent vacancies filled with 2 electrons) shown in Figure 1. While these aggregated F-centers can both be excited with 450 nm light, F_3^+ centers re-emit light

at 525 nm and F_2 centers re-emit light at 650 nm creating two distinct peaks in the emission spectra (Figure 2).

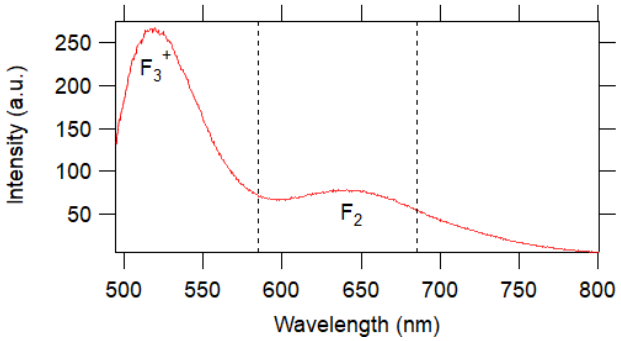

Figure 2: Labeled Emission Spectrum of Gamma Irradiated LiF Sample

2.2. Color Center Kinetics

High energy gamma and neutron radiation can displace ions in the lattice of LiF, primarily creating single F-centers [5]. These F-centers are mobile and can recombine into more complicated color centers such as the F_3^+ and F_2 centers of interest. These kinetics are captured in the following equations from the article: "Color centers aggregation kinetics in lithium fluoride after gamma irradiation"[6]:

$$\nu_a + e \rightarrow F \quad (1)$$
$$\nu_a + F \rightarrow F_2^+ \quad (2)$$
$$F_2^+ + e \rightarrow F_2 \quad (3)$$
$$\nu_a + F_2 \rightarrow F_3^+ \quad (4)$$
$$F_2^+ + F \rightarrow F_3^+ \quad (5)$$

Figure 3: Sample Color Center Kinetic Processes. (ν_a = Anion Vacancy, e = Electron, F = Single F-center, F_x^y = Aggregated Color Center)

Because of these processes, the fluorescence of F_3^+ and F_2 centers can vary over time during and after irradiation. In the samples that were measured in this study, this manifested as an exponential increase in fluorescence at room temperature with time constants unique to color center type and which were proportional to the sample's received dose. Additionally, annealing the samples at high temperatures breaks up the aggregated color centers, eventually reducing the sample's emission spectra to pre-irradiation levels.

3. Methods

3.1. Bulk Fluorescence

The measured LiF samples were 0.5x0.5x0.5 cm^3 crystals provided by United Crystal. The samples were measured with the following scan conditions in a Cary Eclipse Spectrophotometer at room temperature: excitation with a 450 nm band-pass filter, emission measured with a 488 nm long-pass filter, and an overall measured spectral range of 495 to 800 nm. Neutron irradiation was done with an Americium-Beryllium (AmBe) source with an activity of 3.7 GBq and the gamma source was a ^{60}Co source with an activity of 2.8 GBq.

3.1.1 Time Dependence

One sample was gamma irradiated for 3 hours and then measured repeatedly for 43 hours to record the exponential increase in color center fluorescence. The signals were integrated across the F_3^+ (495 - 585 nm) and F_2 (585 - 685 nm) spectral ranges, shown in Figure 2. The integrated fluorescence was fit to exponential curves to calculate time constants.

3.1.2 Annealing Temperature Dependence

Nine samples were analyzed at increasing annealing temperatures. The samples were gamma irradiated for 41.3 hours and stored in vacuum for 72 hours before any measurements to avoid time-dependent fluorescence increase. Annealing was done in an Across International STF1200-50x600 model furnace. The nine samples were annealed separately in 30°C temperature steps from 50°C to 290°C for 1 hour at the desired temperature. The samples were measured before irradiation, pre-annealing , and post-annealing. The pre- and post-annealing spectra were integrated over the color center's respective spectral ranges to calculate the decrease in fluorescence. The study was also repeated with nine samples that were neutron irradiated for 192 hours and annealed in 15°C temperature steps from 50°C to 170°C.

3.2. Track Fluorescence

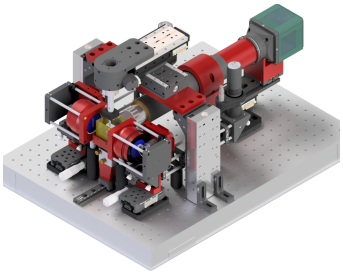

Figure 4: Benchtop mesoSPIM Diagram [3]

A LiF sample was neutron irradiated for 24 hours and scanned with a benchtop mesoSPIM at the University of Zurich. The pixel size was 0.425 x 0.425 μm^2 for each image and the sample step size was 6 μm creating an anisotropic voxel spacing of 0.425 x 0.425 x 6 μm^3. With the current MATLAB data processing method, the data goes through the following steps:

1. A subset of the entire volume that was uniformly illuminated by the excitation laser was selected
2. Gaussian blurring is applied over the selected volume's slices to reduce noise (Figure 5).
3. Morphological top-hat filtering is applied with a disc shaped structuring element to separate bright vacancy pixels from background (Figure 6).
4. A low threshold is applied to the selected volume to find voxels with a brightness slightly above background levels.
5. Track clusters are determined by pixel connectivity.
6. Clusters which have voxels which are above a higher threshold value are kept (Figure 7) and track metrics such as length, total brightness, and direction are calculated.

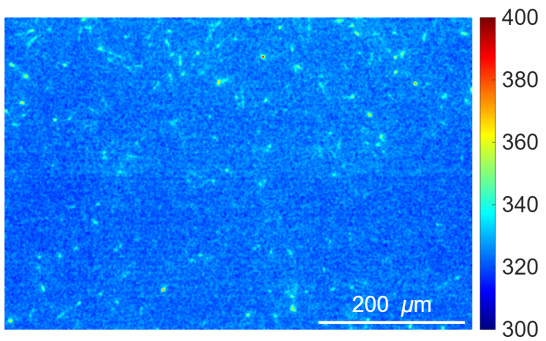

Figure 5: LiF Slice After Gaussian Smoothing

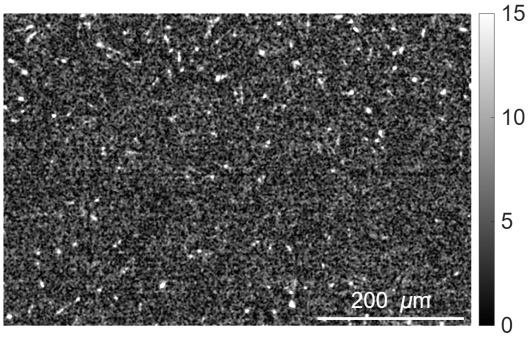

Figure 6: LiF Slice After Top Hat Morphology

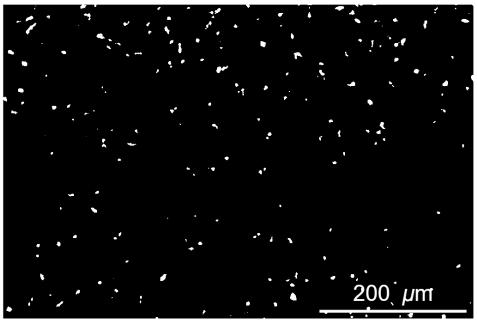

Figure 7: Thresholded Track Pixels

4. Results

4.1. Bulk Fluorescence

4.1.1 Time Dependence

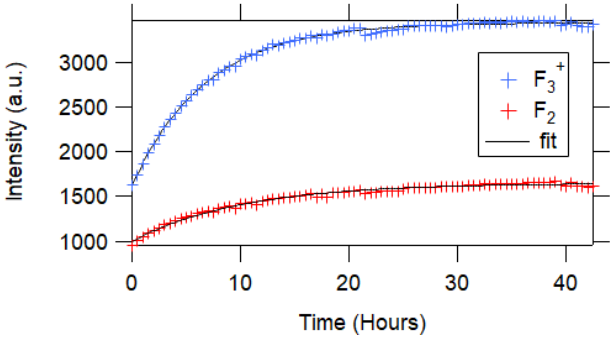

Figure 8: Exponential Increase in F_3^+ and F_2 Integrated Fluorescence Post Gamma Irradiation

For the gamma irradiated samples, the F_3^+ center fit a time constant of 6.8141 ± 0.078 hours and the F_2 center fit a time constant of 10.118 ± 0.31 hours. For the neutron irradiated samples, there seemed to be no significant increase/variation in fluorescence immediately after irradiation indicating that the time constant may be small enough to be ignored.

4.1.2 Annealing Temperature Dependence

For the following plots, "Background" refers to the pre-irradiation spectrum of the sample.

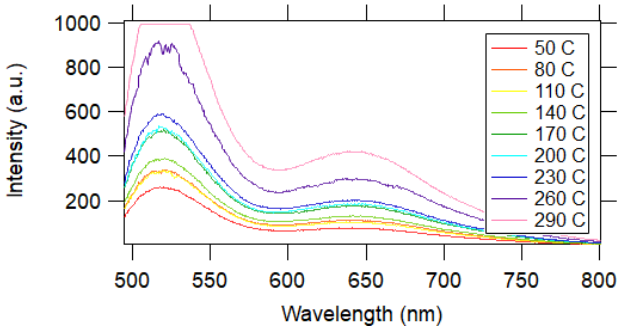

Figure 9: Pre-Annealing Emission Spectra of Gamma Irradiated Samples (Background Subtracted)

Note that in Figure 9, for the pre-annealing F_3^+ spectral range of the sample that underwent annealing at 290°C, the fluorescence saturated the spectrophotometer's photomultiplier tube (PMT). To prevent issues with fitting later, the pre- and post-annealing spectrum of this sample was remeasured with half of the emission slit width to produce plots without saturation issues.

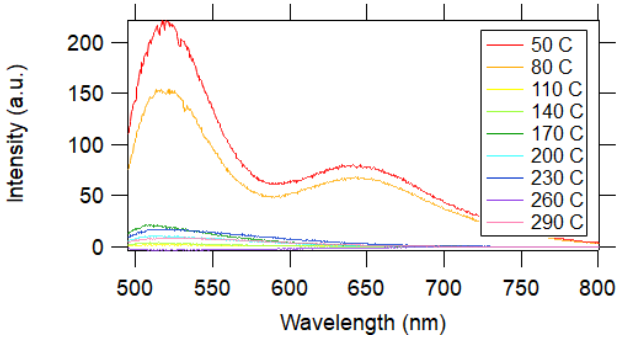

Figure 10: Post-Annealing Emission Spectra of Gamma Irradiated Samples (Background Subtracted)

From Figure 10, the samples which underwent annealing at temperatures higher than 100°C had subtracted spectra close to 0, indicating that most of the gamma radiation damage has been erased.

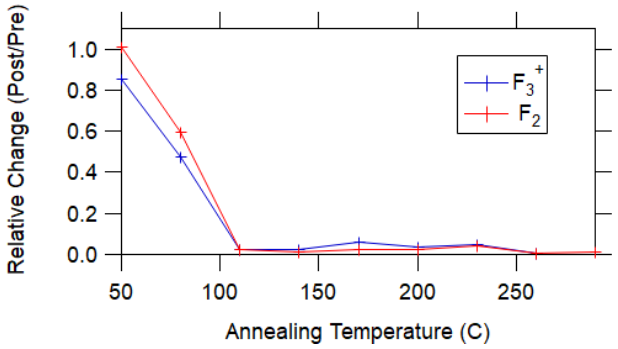

Figure 11: Relative Change in Integrated Fluorescence after Annealing for Gamma Irradiated Samples (Background Subtracted Data)

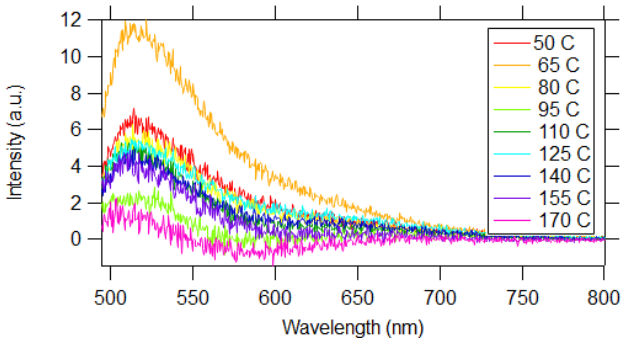

Figure 12: Pre-Annealing Emission Spectra of Neutron Irradiated Samples (Background Subtracted)

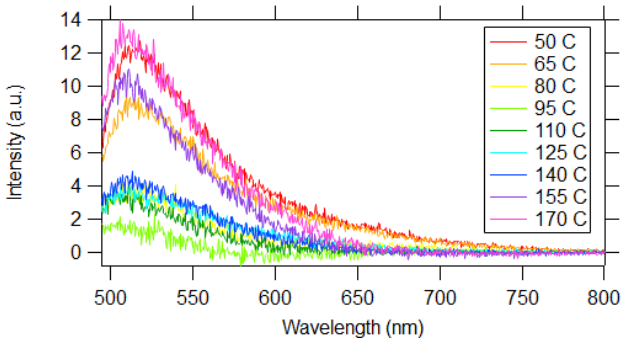

Figure 13: Post-Annealing Emission Spectra of Neutron Irradiated Samples (Background Subtracted)

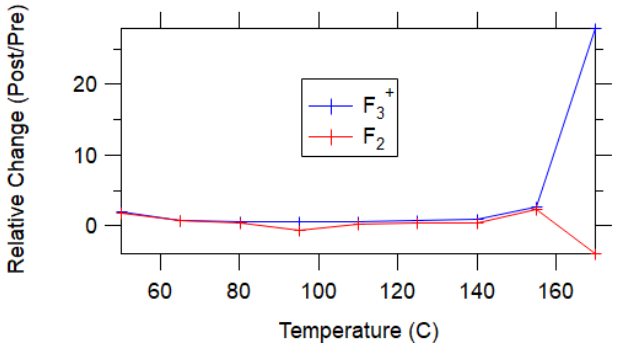

Figure 14: Relative Change in Integrated Fluorescence after Annealing for Neutron Irradiated Samples (Background Subtracted Data)

From the pre-annealing plot (Figure 12), the

sample which was annealed at 170°C has the dimmest emission spectrum. However, in the post-annealing plot (Figure 13) the same sample also had the brightest spectrum leading to issues when calculating the relative change in fluorescence (Figure 14). This issue is why the same dataset was reanalyzed without background subtraction (Figure 15), and is also explored in the discussion section later.

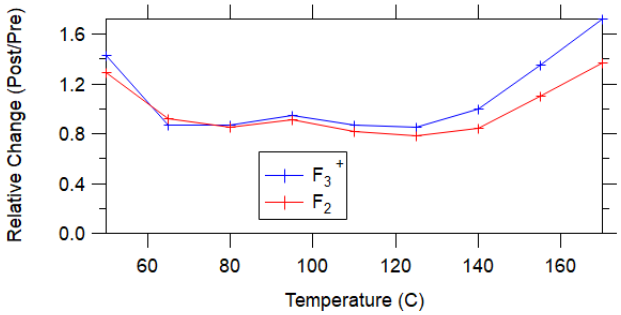

Figure 15: Relative Change in Integrated Fluorescence after Annealing for Neutron Irradiated Samples (No Background Subtraction)

4.2. Track Fluorescence

For the following track analysis, the selected volume was 425 x 637.5 x 108 μm^3.

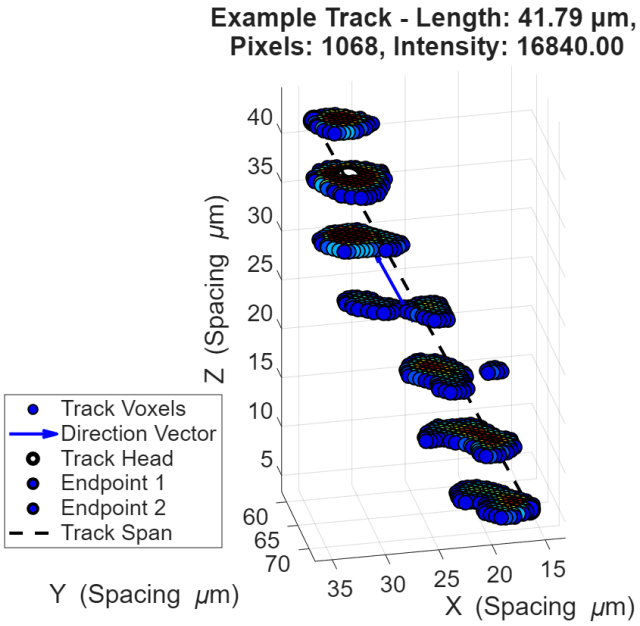

Figure 16: Sample Track in Neutron Irradiated LiF Sample Imaged with Benchtop mesoSPIM

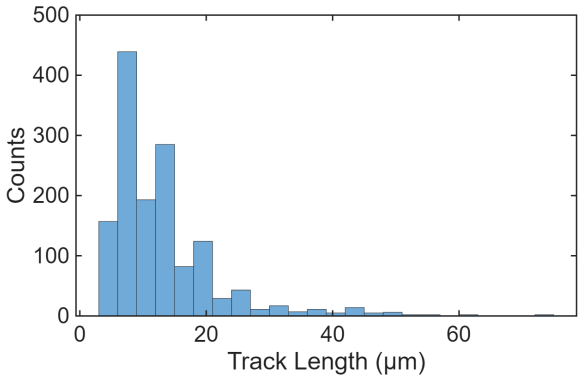

Figure 17: Track Length Histogram in Neutron Irradiated LiF Sample Imaged with Benchtop mesoSPIM

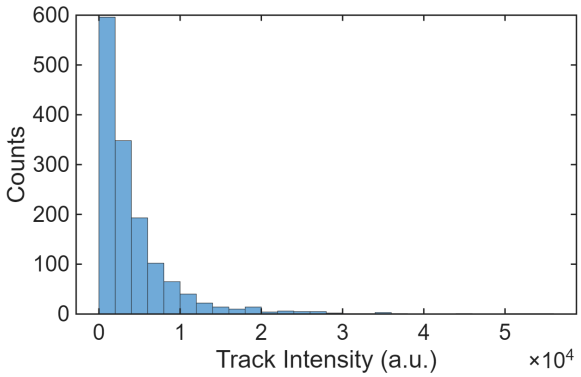

Figure 18: Track Intensity Histogram in Neutron Irradiated LiF Sample Imaged with Benchtop mesoSPIM

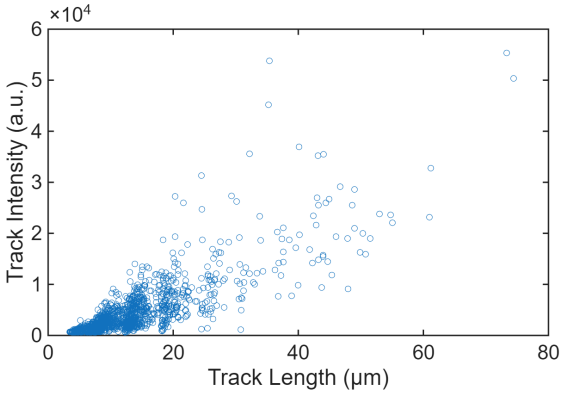

Figure 19: Track Intensity vs Track Length in Neutron Irradiated LiF Sample Imaged with Benchtop mesoSPIM

5. Discussion

5.1. Bulk Fluorescence

5.1.1 Time Dependence

Table 1: Time Constant Comparison (Hours)

Gamma Dose	F_3^+	F_2
3 Hours (This Study)	6.8	10.1
1 Hour (Previous Study)	6.5	9

The calculated time constants were comparable, but slightly higher, than previous results [2]. This could be due to the larger gamma irradiation dose in this study, which leads to a higher initial F-center concentration, increasing the reaction rate of the processes from Figure 3 [6]. However, it is more likely due to measurement/fit uncertainty.

5.1.2 Annealing Temperature Dependence

There was significant variation in the pre-annealing spectra of the gamma irradiated samples. This could be due to anisotropy in the gamma source leading to the 9 samples receiving varying doses. It could also be a result of the larger gamma dose which was used in this study leading to a greater time constant than previously calculated for the 3 hour dose. For these gamma irradiated samples, the annealing results indicate some level of fluorescence decrease at lower temperatures than previously used for complete annealing of LiF radiation damage (350°C).

For the neutron irradiated samples, there was an issue with the sample that was annealed at 170°C due to its pre- and post-irradiation spectra being very similar (Figures 12 and 13). This may have been due to degradation of its optical surface or because the sample did not receive a large neutron dose. The latter is not likely, as the sample's fluorescence greatly increased after annealing, which should be a result of radiation induced color-center formation. This caused issues when plotting the relative change with background subtracted data (the final data point being unrealistically large). However, from the data which is not background subtracted, it is clear that there is an increase in fluorescence for the neutron irradiated samples at low temperatures (∼50°C) and moderately high temperatures (∼160°C). This increase of fluorescence at moderately high temperatures agrees with the results of studies on alpha-particle irradiated LiF samples which have shown that track fluorescence can increase when heated at temperatures ranging from 200°C to 300°C [4]. Future studies could explore the behavior of neutron irradiated LiF fluorescence at higher temperatures to explore whether this fluorescence keeps increasing past 170°C, and when it begins to decrease again.

This difference in behavior of gamma irradiated samples versus neutron irradiated samples could also be utilized for improving LSFM images for neutron track studies. For example, annealing at 170°C seems to greatly reduce gamma fluorescence (Figure 11) but it also enhances neutron fluorescence (Figure 15). Therefore, thermal enhancement at 170°C (or possibly larger temperatures) could improve signal-to-noise ratio in track imaging by suppressing the gamma background in samples which have experienced both radiation types.

5.2. Track Fluorescence

Currently the code uses a region-growing approach to classify tracks, however, this is susceptible to issues from background noise. Additionally, it is apparent from Figure 19 that there are gaps in computed track lengths. This is likely from the anisotropic scan resolution since there are ∼6 μm gaps between clusters in Figure 19, corresponding to the 6 μm z-axis imaging resolution. This could also lead to inaccurate counting in Figure 17, inflating the counts of tracks that have lengths close to multiples of 6 μm. In the future, scans of the same crystal in multiple orientations may allow tracks to be voxelized with higher resolution in all directions, filling in these gaps.

6. Conclusion

We have shown that color center fluorescence manifests very differently between gamma and neutron irradiated samples, through time dependence and temperature dependence studies. This difference in behavior could be leveraged to bias for a specific radiation type. Further development in LSFM imaging and track identification will allow deeper exploration of these processes beyond Bulk Fluorescence studies, in addition to supporting the objectives of the PALEOCCENE collaboration. For example, correlating track shapes to physical processes will be crucial in filtering out known background signals from natural sample searches for dark matter damage.

Acknowledgments

This project was made possible through the support of the National Science Foundation under grant No. PHY-2149165 and the guidance of my mentor Dr. Patrick Huber.

References

[1] Krystal Alfonso et al. Passive low energy nuclear recoil detection with color centers – PALEOCCENE. In *Snowmass 2021*, 3 2022.

[2] Gabriela A. Araujo et al. Nuclear recoil detection with color centers in bulk lithium fluoride. 3 2025.

[3] Nikita Vladimirov et al. Benchtop mesospim: a next-generation open-source light-sheet microscope for cleared samples. *Nature Communications*, 15:2679, 2024.

[4] M. Sankowska, P. Bilski, and B. Marczewska. Thermal enhancement of the intensity of fluorescent nuclear tracks in lithium fluoride crystals. *Radiation Measurements*, 157:106845, 2022.

[5] Małgorzata Sankowska, Pawel Bilski, Barbara Marczewska, and Yaroslav Zhydachevskyy. Influence of elevated temperature on color centers in lif crystals and their photoluminescence. *Materials*, 16(4), 2023.

[6] A.P. Voitovich, V.S. Kalinov, L.P. Runets, A.P. Stupak, E.F. Martynovich, R.M. Montereali, and G. Baldacchini. Color centers aggregation kinetics in lithium fluoride after gamma irradiation. *Journal of Luminescence*, 143:207–214, 2013.